

New limb-darkening coefficients and synthetic photometry for model-atmosphere grids at Galactic, LMC, and SMC abundances.

Ian D. Howarth*

Dept. Physics & Astronomy, UCL, Gower Street, London WC1E 6BT, UK

Accepted. Received; in original form

ABSTRACT

New grids of ATLAS9 models have been calculated using revised convection parameters and updated opacity-distribution functions, for chemical compositions intended to be representative of solar, $[M/H] = +0.3, +0.5$, Large Magellanic Cloud (LMC), and Small Magellanic Cloud (SMC) abundances. The grids cover $T_{\text{eff}} = 3.5\text{--}50\text{kK}$, from $\log g = 5.0$ to the effective Eddington limit. Limb-darkening coefficients and synthetic photometry are presented in the *UBVRIJHKLM*, *wby*, *ugriz*, WFCAM, Hipparcos/Tycho, and Kepler passbands for these models, and for Castelli’s comparable ‘new-ODF’ grids. Flux distributions are given for the new models. The sensitivity of limb-darkening coefficients to the adopted physics is illustrated.

1 INTRODUCTION

The significance of limb darkening as a probe of atmospheric structure was recognized from the earliest modelling of stellar atmospheres (e.g., Schwarzschild 1906; Jeans 1917; Milne 1921), and its importance in the quantitative photometric analysis of eclipsing binaries similarly noted (Russell 1912; Russell & Shapley 1912). Reliable empirical determinations of limb darkening are rarely possible in eclipsing binaries (in part because of degeneracies with other parameters), and so values derived from model-atmosphere calculations retain their importance through to the present day, where new applications include modelling of exoplanetary transits, microlensing events, and spatially resolved stellar surfaces (e.g., Southworth 2008; Witt 1995; Hestroffer 1997; Aufdenberg, Ludwig & Kervella 2005).

Wholesale calculation of limb-darkening coefficients became feasible only after production of the first large grids of model atmospheres (cf. Grygar, Cooper & Jurkevich 1972, who review earlier studies). In particular, the extensive model-atmosphere grids generated by Kurucz (1979, 1993) form the basis of work by Wade & Rucinski (1985), Díaz-Cordovés & Giménez (1992), van Hamme (1993), Claret (2000), and others.

Although several programs are now available in the public domain for generating line-blanketed model atmospheres which relax the approximation of Local Thermodynamic Equilibrium (LTE), Kurucz’s ATLAS codes remain the benchmark for LTE calculations, and have two major attractions for the present purposes. First, while the models may not accurately reproduce individual spectral lines for which non-LTE effects are significant, they nonetheless appear to be quite successful in generating accurate atmospheric structures and broad-band fluxes.

Secondly, it is straightforward, and computationally

cheap, to generate self-consistent ATLAS grids covering large ranges in parameters of interest. The aspect of internal consistency is of particular importance when modelling the spectra of systems whose temperatures and gravities may show considerable variations over their surfaces (such as the components of close binary systems, rapidly rotating stars, and non-radial pulsators), and when attempting uniform analyses of samples encompassing a range of stellar parameters (for example, in synoptic studies of light-curves of exoplanetary transits).

Almost all extensive calculations of grids of ATLAS-based limb-darkening coefficients published to date have used the formulations of opacity-distribution functions (ODFs) and atmospheric convection inherent to the models published by Kurucz (1993).¹ However, improved treatments in both areas have emerged subsequently, leading in some cases to quite significant changes in the models (Castelli & Kurucz 2004). The principal purpose of the present paper is to present calculations of limb-darkening coefficients made using new ODFs and improved parameterizations of convection. Because of growing interest in modelling eclipsing binaries in the Magellanic Clouds (e.g., Harries, Hilditch & Howarth 2003; Hilditch, Howarth & Harries 2005; Bonanos 2000; North et al. 2010), new models with tailored MC abundances are included.

2 MODELS

ATLAS has undergone more or less continuous development over its ~ 40 -year lifetime, and currently ex-

¹ An exception is work reported by Barban et al. (2003)

ists in two distinct forms, ATLAS9 (which uses opacity-distribution functions) and ATLAS12 (which uses opacity sampling). The models discussed here were all computed using the Trieste port of ATLAS9 to GNU-linux systems (Sbordone, Bonifacio & Castelli 2007).

2.1 ODFs and Abundances

Opacity-distribution functions are required as a basic input to ATLAS9 models. Castelli & Kurucz (2004) describe ODFs which incorporate a variety of improvements over those used in the Kurucz (1993) grids, of which perhaps the most important is the inclusion of improved and additional molecular opacities. The models described here use new ODFs, generated using DFSYNTH (Kurucz 2005; Castelli 2005), based on the Castelli & Kurucz (2004) line lists.

The baseline models use solar abundances reported by Asplund, Grevesse & Sauval (2005). Limb darkening plays an important role in the analysis of light-curves of stars with transiting exoplanets, and the sample of such stars currently known shows a propensity for enhanced metallicity (e.g., Gonzalez 1997; Fischer & Valenti 2005; Sousa et al. 2008). With this in mind, additional models (and ODFs) were calculated with metallicities enhanced by +0.3 and +0.5 dex over solar values. For test purposes, ODFs (but not model grids) were computed at several other metallicities, including $[M/H] = -0.5$ for the Vega models discussed in Section 5.

The routine study of eclipsing binaries in external galaxies, and especially in the Magellanic Clouds (MCs), has become feasible in recent years. While no one set of MC abundances is likely to be generally satisfactory, most interest in eclipsing binaries in the Clouds has concentrated on early-type stars (in part because of their intrinsic brightness). In order to have an appropriate (Pop. I) reference set of representative Large and Small Magellanic Cloud abundances that are at least well defined, and apparently reasonable, results have been compiled from a number of sources. These abundances, listed in Appendix A (Table A1), have been used to compute new LMC and SMC ODFs.

All the ODFs newly calculated here are available online.

2.2 Convection

All model-atmosphere codes incorporate approximations and parameterizations of physics that may be difficult or expensive to model, or is simply poorly understood (cf., e.g., Kurucz 1996). Convection is a prime example, and is characterized in ATLAS9 by a mixing-length approximation with optional overshooting.

The widely distributed Kurucz (1993) grids were calculated with a ratio of mixing length to pressure scale height of $\ell/H = 1.25$ and overshooting included, but Castelli, Gratton & Kurucz (1997) argue that more-consistent results are obtained with ATLAS9 when overshooting is switched off. Furthermore, Smalley (2005, and personal communication) advocates smaller values of the mixing-length parameter over at least the late-A spectral range.

All the models presented here were calculated with no overshooting. The baseline grids use $\ell/H = 1.25$, but supplementary grids at $\ell/H = 0.50$ were also computed.

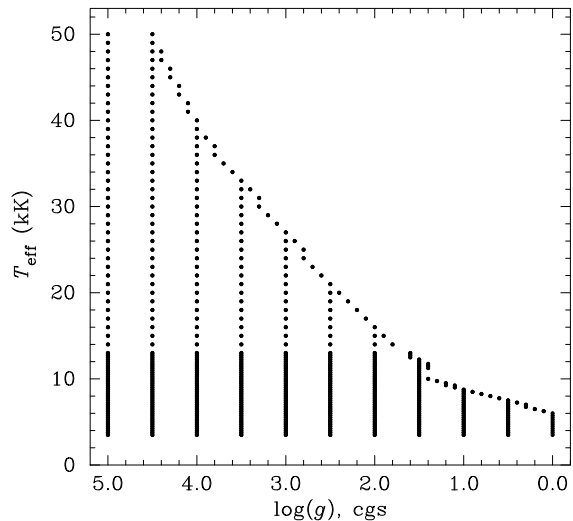


Figure 1. Grid for solar-abundance models (the lowest gravities may be 0.1–0.2 dex larger at higher metallicities).

2.3 Parameter space

The grid sampling adopted here matches the basic $T_{\text{eff}}/\log g$ sampling of the Castelli & Kurucz (2004) models; that is, from 3.5–13kK at 0.25kK intervals, and 12.0–50.0kK at 1kK intervals, from $\log g = 5.0$ dex (cgs) to lower values at 0.5-dex intervals. This grid density is sufficient for interpolation of output products (e.g., linearly in $\log T_{\text{eff}}/\log g$) to be satisfactory for most applications. Some effort has been put into generating models to as low a gravity as possible at a given temperature (the effective Eddington limit), and so the present grids extend beyond Castelli & Kurucz’s in this regard. The sampling is illustrated in Fig. 1.

Previous work suggests that the ATLAS9 turbulent-velocity parameter v_t has little consequence for limb-darkening in the optical regime, and its value (as well as its physical significance) is difficult to establish observationally in any individual case. Most of the model intensities presented here have been computed with a canonical $v_t = 2 \text{ km s}^{-1}$. Solar-abundance grids at $v_t = 0$ and 4 km s^{-1} confirm the insensitivity of limb darkening to v_t .

Results of grids of 6571 new models are presented here. Castelli & Kurucz (2004) have calculated models using solar abundances listed by Grevesse & Sauval (1998), which differ only slightly from those given by Asplund, Grevesse & Sauval (2005). Their grids extend over a greater range in scaled solar abundances than those newly calculated here, and include additional modifications to abundances of alpha-process elements. For completeness, intensities have also been calculated from the 8568 atmospheric structures they provide, along with limb-darkening coefficients and other products to match the new grids. Table 1 summarizes the grids, where ‘ATLAS9.C04’ and ‘ATLAS9.A10’ identify the Castelli & Kurucz (2004) and current grids, respectively.

3 DATA PRODUCTS

The principal motivation for the work reported here was to provide up-to-date limb-darkening coefficients (particularly

Table 1. Summary of ATLAS9 models. The sources for the atmospheric structures are Castelli & Kurucz (2004; ATLAS9.C04) and the present paper (ATLAS9.A10). In the ‘Grid’ columns, with entries of the form ‘xIIvJJ’, ‘xII’ indicates the scaling applied to metals from the default solar abundance (such that ‘m10’ indicates a metallicity $[M/H] = -1.0$, and ‘p05’ $+0.5$), while ‘vJJ’ indicates the turbulent velocity used in the model (‘JJ’ in km s^{-1}). Models at LMC and SMC abundances are so labelled. The quantity ℓ/H is ratio of mixing length to pressure scale height. The number of models in a given grid, N , is greater for the ATLAS9.A10 set because these generally extend to somewhat lower gravities than the ATLAS9.C04 calculations, at all 76 grid temperatures.

Structure source	Grid	ℓ/H	N	Grid	ℓ/H	N
ATLAS9.C04	m25v02	1.25	476	m40av02	1.25	476
ATLAS9.C04	m20v02	1.25	476	m25av02	1.25	476
ATLAS9.C04	m15v02	1.25	476	m20av02	1.25	476
ATLAS9.C04	m10v02	1.25	476	m15av02	1.25	476
ATLAS9.C04	m05v02	1.25	476	m10av02	1.25	476
ATLAS9.C04	p00v00	1.25	476	m05av02	1.25	476
ATLAS9.C04	p00v02	1.25	476	p00av02	1.25	476
ATLAS9.C04	p02v02	1.25	476	p02av02	1.25	476
ATLAS9.C04	p05v02	1.25	476	p05av02	1.25	476
ATLAS9.A10	P00v00	1.25	554	LMCv02	1.25	554
ATLAS9.A10	P00v02	1.25	554	LMCv02r	0.50	552
ATLAS9.A10	P00v02r	0.50	552	SMCv02	1.25	554
ATLAS9.A10	P00v04	1.25	548	SMCv02r	0.50	552
ATLAS9.A10	P03v02	1.25	543			
ATLAS9.A10	P03v02r	0.50	544			
ATLAS9.A10	P05v02	1.25	531			
ATLAS9.A10	P05v02r	0.50	533			

at MC abundances). Thus the main data products are specific intensities (monochromatic radiances) $I_\lambda(\mu)$, as a function of μ , the cosine of the angle between the line of sight and the surface normal. These are provided in condensed form as broad-band limb-darkening coefficients.

Physical fluxes,

$$F_\lambda = 2\pi \int_0^1 I_\lambda(\mu) \mu \, d\mu = 4\pi H_\lambda \quad (1)$$

(where H_λ is the Eddington flux), are required as a check on the accuracy of intensity integrations, and in any case represent only a minor additional computational overhead. Model fluxes are therefore also provided, both at the 1221 wavelengths used in the structure calculations (91Å–160μm), and in broad-band (‘synthetic photometry’) form. Other data products (such as model structures and higher-resolution intensities) will be made freely available on request.

4 LIMB DARKENING

4.1 Passbands

Modern detectors working in the optical are essentially photon-counting in nature. For such detectors broad-band model intensities (and, *mutatis mutandis*, fluxes) may be calculated as

$$I_i(\mu) = \frac{\int_\lambda I_\lambda(\mu) \phi_\lambda(i) \lambda \, d\lambda}{\int_\lambda \phi_\lambda(i) \lambda \, d\lambda}, \quad (2)$$

(e.g., Bessell 2005) where $\phi_\lambda(i)$ is the response function of passband i in a given photometric system. Historically, the equivalent formalism for energy-integrating detectors has

been used:

$$I_i(\mu) = \frac{\int_\lambda I_\lambda(\mu) \phi_\lambda(i) \, d\lambda}{\int_\lambda \phi_\lambda(i) \, d\lambda}. \quad (3)$$

Results are provided for photon-counting detectors for all photometric systems considered here, and additionally for energy-integrating detectors for the Johnson and Strömgren passbands. The adopted sources for response functions are:

- *UBVRI* (Johnson–Cousins system): Bessell (1990).
- *JHKLL’M* (Johnson–Glass system): Bessell & Brett (1988).
- *uvby* (Strömgren system): Crawford & Barnes (1970; filters), Stubbs et al. (2007; atmospheric transmission), Hamamatsu (1999; S4 response), Allen (1976, p. 108; aluminium reflectivity), Praezisions Glas & Optik (BK7 glass transmission).²
- *ZYJHK* (WFCAM system): Hewett et al. (2006)
- H_p , B_T , V_T (Hipparcos/Tycho system): Bessell (2000)
- *ugriz* (Sloan system): on-line, <http://www.sdss3.org/instruments/camera.php>
- *Kepler*: on-line, http://keplergo.arc.nasa.gov/kepler_response_hires1.txt

Simple geometric treatments of mutual irradiation (the ‘reflection effect’) in binary-star systems require the angular dependence of the bolometric intensity (Wilson 1990), so bolometric limb-darkening coefficients have also been calculated ($\phi_\lambda \equiv 1$).

² The Strömgren system is close to being filter defined, but atmospheric transmission, 1P21-S4 photomultiplier sensitivity, and BK7 glass transmission all make roughly equal inroads into the short-wavelength edge of the u passband.

4.2 Analytical characterization

Specific intensities are traditionally, and conveniently, characterized by simple functional forms, of which the most venerable is the linear limb-darkening law

$$I(\mu)/I(1) = 1 - u(1 - \mu), \quad (4)$$

the analytical solution for a source function that is linear in optical depth τ (Schwarzschild 1906, Milne 1921; $u = 0.6$ for a grey atmosphere).

More-realistic models do not have analytical solutions, and additional terms are required for a faithful functional representation of actual limb darkening. Kopal (1949) took a series-expansion approach, and found the differences between quadratic and quartic approximations to be negligible at the level of accuracy with which he was concerned. Two-coefficient parameterizations subsequently became standard; in particular, a quadratic law of the form

$$I(\mu)/I(1) = 1 - a(1 - \mu) - b(1 - \mu)^2 \quad (5)$$

was widely adopted in the modern computational era (e.g., Manduca, Bell & Gustafsson 1977; Wade & Rucinski 1985), although a cubic version,

$$I(\mu)/I(1) = 1 - a(1 - \mu) - b(1 - \mu)^3,$$

was advocated by van 't Veer (1960). An alternative logarithmic law,

$$I(\mu)/I(1) = 1 - a(1 - \mu) - b(\mu \ln \mu) \quad (6)$$

was proposed by KlingleSmith & Sobieski (1970), and a square-root law,

$$I(\mu)/I(1) = 1 - a(1 - \mu) - b(1 - \sqrt{\mu}), \quad (7)$$

by Díaz-Cordovés & Giménez (1992).

For modern work, these limb-darkening laws suffer from various limitations. The obvious way to develop a single analytical expression that more accurately reproduces numerical limb-darkening results across a wide parameter space is simply to use more terms, a notion implemented by Claret (2000) who introduced a four-coefficient fit in powers of $\sqrt{\mu}$,

$$I(\mu)/I(1) = 1 - \sum_{n=1}^4 a_n \left(1 - \mu^{n/2}\right). \quad (8)$$

Figure 2 illustrates the differing degrees to which the foregoing common functional forms reproduce the intensities computed here. While quantitative results depend on the chosen normalization and adopted figure of merit, the qualitative conclusions are robust: a linear limb-darkening law is a rather poor representation of detailed numerical results; a quadratic law fares little better; but the four-coefficient law affords an improvement of up to an order of magnitude in precision over any standard two-coefficient option. While there has been some discussion in the literature as to which is the most appropriate limb-darkening ‘law’ to adopt for light-curve analyses, and in particular under circumstances which permit empirical determination of limb-darkening coefficients (e.g., Southworth 2008), there seems little justification for adopting anything other than a high-order fit such as eqn. (8) if the principal purpose is to secure an accurate representation of model-atmosphere results.

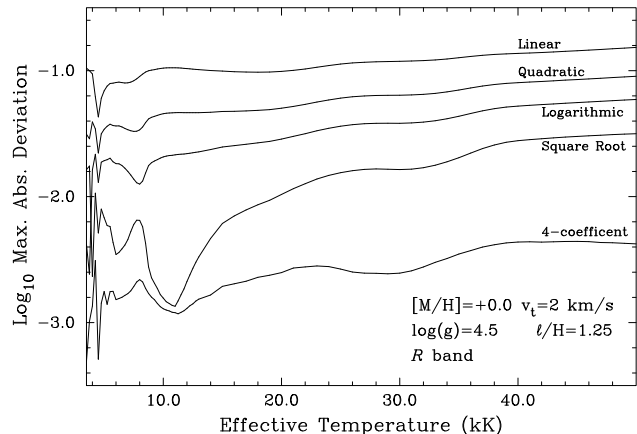


Figure 2. Comparison of different parameterizations of limb darkening (equations 4–8). The quantity plotted is \log_{10} of the maximum absolute difference between input and parameterized values of $I(\mu)/I(1)$.

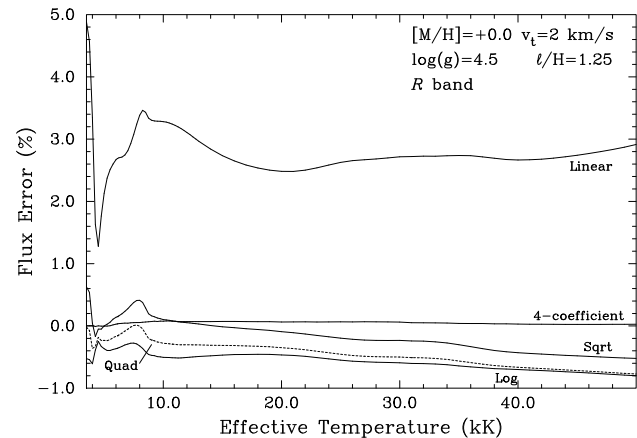


Figure 3. Differences, flux minus integrated intensity (expressed as a percentage of flux) for several limb-darkening laws (see Section 4.3).

4.3 Fitting procedure

For any given analytical form, there remains a choice of numerical technique for determining the limb-darkening coefficients. The most direct approach is simple least-squares determination of coefficients from functional fits to computed $I(\mu)$ values (with $\hat{I}(1)$, the fitted value of $I(1)$, as an optional additional free parameter). A related approach, the r -integration method (Heyrovský 2007), appears to offer no significant benefits (Claret 2008).

A criticism that can be levelled against the least-squares method is that subsequent integration of parameterized intensities may not accurately recover the flux, as it should (eqn. 1). Alternative formulations in which flux is explicitly conserved can be devised (e.g., Wade & Rucinski 1985; van Hamme 1993), giving rise to so-called flux conservation methods (cf., e.g., Claret 2008, for a recent discussion). Such methods require some further *ad hoc* constraint; e.g., Wade & Rucinski (1985) set $\hat{I}(1) \equiv I(1)$ for the linear model.

For the most part, straightforward least-squares fitting

has been used here, to intensities evaluated at 20 angles.³ Subsequent analytical integration of the four-coefficient intensity model then reproduces directly computed fluxes to better than 0.1%. When fit in this manner, all two-coefficient models conserve flux to within $\sim 1\%$, while the linear model again fares poorly (Fig. 3).

5 PHOTOMETRIC MATTERS

Broad-band fluxes have potential utility in a variety of applications (effective-temperature determinations, population synthesis, etc.). Thus while it is not the intention here to conduct a detailed confrontation of the new model fluxes with observations, a basic transformation of the synthetic photometry to observed magnitude systems may be of interest. Modern systems generally have dedicated programmes of flux calibration, so the focus here is on the Johnson and Strömberg systems.

5.1 Johnson system

5.1.1 Flux zero-point

Full normalization of the synthetic photometry can be divided into two parts: absolute flux calibration, and differential (colour) calibration. The former aspect is traditionally bound to the absolute flux calibration of Vega, which has been addressed in detail by Hayes (1985) and Mégessier (1995), using primary measurements mostly made in the 1970s. Their key results can be summarized as pseudo-monochromatic 5556-Å fluxes:

$$\begin{aligned} f(5556) &= 3.44 \times 10^{-9} && \text{erg cm}^{-2} \text{ s}^{-1} \text{ \AA}^{-1} \\ &3.46 \times 10^{-11} && \text{W m}^{-2} \text{ nm}^{-1} \end{aligned}$$

respectively. These results can be used to provide a zero-point calibration for the present grids by using a model matching Vega, and its observed V -band magnitude.

Both ‘the’ V -band magnitude, and the choice of model, are subject to uncertainty; widely adopted values are $V = 0.03$ (Johnson et al. 1966), and $T_{\text{eff}} = 9550\text{K}$, $\log g = 3.95$, $[\text{M}/\text{H}] = -0.5$, $v_t = 2 \text{ km s}^{-1}$ (Castelli & Kurucz 1994). Subsequent analyses have supported this effective temperature (e.g. Ciardi et al. 2001; Hill, Gulliver & Adelman 2010), but the HST calibration programme uses a model with $T_{\text{eff}} = 9400\text{K}$, $\log g = 3.90$, $[\text{M}/\text{H}] = -0.5$, $v_t = 0 \text{ km s}^{-1}$ (Bohlin 2007). Workers are therefore faced with choices in observed flux, observed magnitude, and adopted model, as well as in whether to adopt energy-integrating or photon-counting magnitudes. The situation is further complicated by the fact that Vega is a rapid rotator viewed pole-on (Gray 1988; Gulliver et al. 1991; Aufdenberg et al. 2006; Hill, Gulliver & Adelman 2010), so that in principle no single-temperature model can give an accurate representation of the entire flux distribution (although for magnitude zero-point calibration this is of minor importance, because the models are only used to scale between 5556-Å and V -band fluxes).

³ For comparison purposes, the linear law has been modelled with and without $I(1)$ as an optimized parameter, and with explicit flux conservation; Appendix B.

The baseline adopted here is the Hayes calibration, 9.55kK model, Johnson et al. (1966) V , and photon-counting magnitudes. For this system the V -band flux $f(V)$ is $1.031 \times f(5556)$, yielding

$$\begin{aligned} V &= -2.5 \log_{10} f(V) - 21.096 \\ &+ C_1 + C_2 + C_3 + C_4 \end{aligned} \quad (9)$$

where $f(V)$ is in $\text{erg cm}^{-2} \text{ s}^{-1} \text{ \AA}^{-1}$ and the optional correction factors are

$$\begin{aligned} C_1 &= -0.0004 \text{ for the } T_{\text{eff}} = 9400 \text{ K model;} \\ C_2 &= +0.0063 \text{ for the Mégessier (1995) } f(5556) \text{ flux;} \\ &\text{more generally, } C_2 = 2.5 \log_{10}[f(5556)/f(\text{Hayes})]; \\ C_3 &= +0.0135 \text{ for energy-integrated photometry;} \text{ and} \\ C_4 &= V_{\text{Vega}} - 0.03. \end{aligned}$$

5.1.2 Colour-index zero-points

Differential normalization relies on relating the observed colours of a standard star, or stars, to model fluxes. A model colour index is formed from fluxes in two passbands $P1$ and $P2$ by

$$\begin{aligned} (P1 - P2)_{\text{M}} &= -2.5 \log_{10} \left[\frac{f(P1)}{f(P2)} \right] + (C_{P1} - C_{P2}) \\ &\equiv -2.5 \log_{10} \left[\frac{f(P1)}{f(P2)} \right] + Z_{P12} \end{aligned} \quad (10)$$

where $f(P1), f(P2)$ are model broad-band fluxes and C_{P1}, C_{P2}, Z_{P12} are constants. Equating the right-hand side of eqn. (10) with the observed (reddening-free) colour index yields the required normalizing constant Z_{P12} .

Vega has traditionally been adopted as the primary calibrating star, with increasing use of Sirius as a supplementary standard since the work of Cohen et al. (1992). Once again, however, observed photometry is subject to both statistical uncertainties and deterministic changes (e.g., one might choose to *define* Vega to have colour indexes of zero, or to average values from an ensemble of standard stars), and the appropriate model parameters are also moot. Here the photometry compiled by Bessell, Castelli & Plez (1998) is adopted, as are the Sirius model parameters due to Kurucz which they quote: $T_{\text{eff}} = 9.85\text{kK}$, $\log g = 4.25$, $[\text{M}/\text{H}] = +0.5$, $v_t = 2 \text{ km s}^{-1}$ (see also Castelli 1999). These parameters are in good agreement with other recent determinations (e.g., Hill & Landstreet 1993; van Noort 1998; Qiu et al. 2001).

The resulting normalizing constants are listed in Table 2. Agreement between the Vega and Sirius calibrations for the normalizing constants inferred from the specific set of observed colours adopted here is better for the 9.55kK Vega model, and the adopted Z_{P12} values are the average of this model and the Sirius results.

5.1.3 Bolometric corrections

From the basic definitions of bolometric correction and magnitude, it is straightforward to show that the bolometric correction in some passband P for a model at effective tem-

Table 2. Johnson colour-index normalizations. Column 2 gives the colour zero-point computed from the Vega 9.55kK model, with photometry adopted from Bessell, Castelli & Plez (1998; e.g., observed $(V - R) = -0.009$). Column 3 gives the equivalent results for Sirius. The recommended zero-points, Z_{P12} , are the average of the previous two columns (with corrections for alternative photometries dropped); synthetic colours may then be computed from model fluxes by using eqtn. (10).

C_E is the correction to be added to columns 2–4 for energy-integrating detectors, and $C_{9.4}$ is the correction to be added to column 2 to obtain results for the 9.40kK Vega model. The U_X and B_X passbands are those recommended by Bessell (1990) for use in computing synthetic colours to be compared with observed $(U - B)$ colours.

Colour	Vega 9.40kK	Sirius 9.85kK	Z_{P12}	C_E	$C_{9.4}$
$(U_X - B_X)$	$-0.422 + [(U - B) - 0.000]$	$-0.418 + [(U - B) + 0.045]$	-0.420	$+0.031$	$+0.020$
$(B - V)$	$+0.609 + [(B - V) - 0.000]$	$+0.608 + [(B - V) + 0.010]$	$+0.608$	$+0.000$	$+0.007$
$(V - R)$	$+0.568 + [(V - R) + 0.009]$	$+0.575 + [(V - R) + 0.010]$	$+0.572$	$+0.018$	$+0.005$
$(V - I)$	$+1.260 + [(V - I) + 0.005]$	$+1.276 + [(V - I) + 0.016]$	$+1.268$	-0.002	$+0.010$
$(V - K)$	$+4.924 + [(V - K) - 0.020]$	$+4.918 + [(V - K) + 0.061]$	$+4.921$	-0.002	$+0.026$
$(J - K)$	$+2.261 + [(J - K) - 0.010]$	$+2.249 + [(J - K) + 0.018]$	$+2.255$	-0.002	$+0.006$
$(H - K)$	$+1.156 + [(H - K)]$	$+1.152 + [(H - K) + 0.009]$	$+1.152$	$+0.002$	$+0.002$
$(K - L)$	$+1.872 + [(K - L) - 0.010]$	$+1.872 + [(K - L) - 0.003]$	$+1.872$	-0.001	$+0.002$

perature T_{eff} is given by

$$BC(P) = M_{\text{Bol},\odot} - 2.5 \log_{10} \left[\frac{d_{10}^2}{T_{\odot}^4 R_{\odot}^2} \right] - 2.5 \log_{10} T_{\text{eff}}^4 + 2.5 \log_{10}(f_P) + C_P \quad (11)$$

where d_{10} is 10 pc (expressed in the same units as the solar radius, R_{\odot}) and C_P is the magnitude-normalizing constant, which can be found for the Johnson passbands from data summarized in the preceding two subsections.⁴

Bolometric corrections in the main Johnson bands are included for each model in the on-line listings, adopting $M_{\text{Bol},\odot} = +4.74$. As a check on results, a solar-like model was calculated with $T_{\text{eff}} = 5778\text{K}$, $\log g = 4.44$ (cgs), $v_t = 2 \text{ km s}^{-1}$, $\ell/H = 1.25$, $[M/H] = 0.0$; for this model, the (photon-counting) V -band bolometric correction is found to be $BC(V) = -0.075$, in excellent agreement with the empirical solar value of -0.07 (Bessell, Castelli & Plez 1998).

5.2 A Strömgren calibration

Flux calibration is readily carried out for the Strömgren $uvby$ system in the same way as for the Johnson system. A potential complication is that for the intermediate-width passbands of this system, individual spectral features may be significant; in particular, $H\delta$ (410nm) falls in the middle of the v band. To check that the standard 20-Å spectral sampling is adequate in these circumstances, high-resolution synthetic spectra were computed from the Vega models. Strömgren-band fluxes from these synthetic spectra agree with the standard results to better than 0.1% for u , b , and y , and are only 0.5% smaller at v . Since the Balmer lines reach their greatest strength at early-A spectral types, the standard sampling appears to be satisfactory.

Results are summarized in Table 3. Strömgren colours

can be generated from the models with

$$(b - y) = -2.5 \log_{10} \left[\frac{f(b)}{f(y)} \right] + Z_{by}$$

$$m_1 = -2.5 \log_{10} \left[\frac{f(v) \times f(y)}{f^2(b)} \right] + Z_{m1}$$

$$c_1 = -2.5 \log_{10} \left[\frac{f(u) \times f(b)}{f^2(v)} \right] + Z_{c1}$$

where $f(p)$ is the model flux in passband p and the zero-points Z are the last three entries in column 2 of Table 3.

Fabregat & Reig (1996) and Gray (1998) have previously provided Strömgren flux calibrations which are the results of convolving the $uvby$ passbands with observed spectrophotometry,⁵ from Glushneva et al. (1992) and Taylor (1984), respectively (both nominally on the Hayes 1985 system). Comparison with their results, expressed as a zero-magnitude flux in units of $10^{-9} \text{ erg cm}^{-2} \text{ s}^{-1} \text{ \AA}^{-1}$ for consistency with their presentations, shows generally good agreement:

Band	FR	Gray	Atlas9.A10
u	11.80	11.72	12.20
v	8.69	(8.66)	8.73
b	5.84	5.89	5.90
y	3.69	3.73	3.72

The ~4% difference at u between spectrophotometric and model results may be a consequence of uncertainties in observed Vega magnitudes, which range over 10% in this passband (Perry 1969; Barry 1969; Johansen & Gyldenkerne 1970; Crawford & Barnes 1970); e.g., using Sirius as the calibrator yields a zero-magnitude u -band flux of $11.79 \times 10^{-9} \text{ erg cm}^{-2} \text{ s}^{-1} \text{ \AA}^{-1}$.

6 DISCUSSION

Much attention has been paid in the literature as to which is the best analytical representation of limb darkening, and

⁴ E.g., $C_B \equiv (C_B - C_V) + C_V = +0.608 - 21.096 = -20.488$, where numerical values for photon-counting photometry are from Table 2 and eqtn. (9).

⁵ The Gray v -band calibration is model-based.

Table 3. Summary of Strömgren photometric calibrations (see Section 5.2). The second column gives flux-calibration and colour zero-points for photon-counting detectors, using a $T_{\text{eff}} = 9.55\text{kK}$ model, Crawford & Barnes (1970) photometry and the Hayes (1985) flux calibration for Vega.

C_1 is the correction to be added to the values in column 2 if adopting other sources of photometry;

C_2 is the correction to be added for energy-integrating detectors;

C_3 is the correction to be added for the Mégessier (1995) flux calibration.

Column 6 gives the corrections to be added for a $T_{\text{eff}} = 9.40\text{kK}$ Vega model, while the final column gives the corrections for Sirius photometry (baseline data from Crawford, Barnes & Golson 1970) and a 9.85kK model, where $\Delta V \equiv V_{\text{Vega}} - 0.03$.

Band/ Colour	Vega 9.55kK	C_1	C_2	C_3	Vega 9.40kK	Sirius 9.85kK
u	-19.784	$+(u - 1.445)$	+0.001	+0.0063	-0.045	$+\Delta V - 0.037 + (u - 1.298)$
v	-20.147	$+(v - 0.195)$	+0.000	+0.0063	-0.016	$+\Delta V - 0.019 + (v - 0.166)$
b	-20.573	$+(b - 0.034)$	+0.001	+0.0063	-0.011	$+\Delta V + 0.012 + (b - 0.036)$
y	-21.074	$+(V - 0.03)$	+0.002	+0.0063	-0.006	$+\Delta V - 0.002$
$(b - y)$	-0.500	$+0.004 - (b - y)$	+0.000		+0.004	$-0.015 + [0.006 - (b - y)]$
m_1	+0.074	$+0.157 - m_1$	+0.001		+0.001	$+0.047 + [0.124 - m_1]$
c_1	+0.064	$+1.089 - c_1$	-0.002		+0.023	$-0.015 + [1.002 - c_1]$

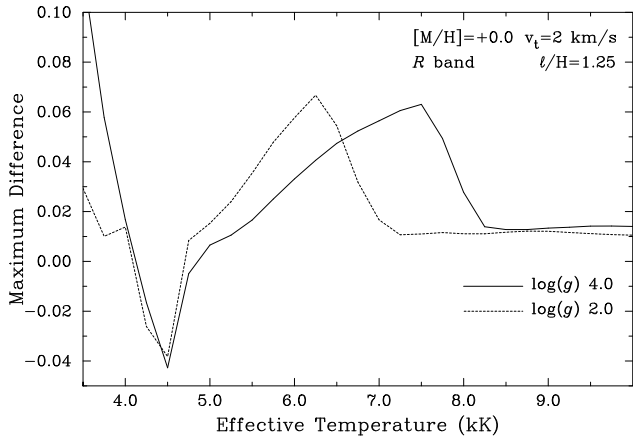


Figure 4. Maximum differences in $I(\mu)/I(1)$ between the results of the present models and fits by Claret (2000) to earlier Kurucz models.

which is the appropriate numerical technique for evaluating limb-darkening coefficients (see discussion and references in Sections 4.2, 4.3). While these are important details, the use of a high-order parameterization, which provides satisfactory results under most circumstances, renders such details academic.

However, the larger importance of the underlying model atmospheres has not generally been emphasized, perhaps because most analysts have used ‘off-the-shelf’ model-atmosphere results. The new opacity sources introduced in the Castelli & Kurucz (2004) models show up directly in emergent fluxes and intensities, and the changes in treatment of convection also change the structures. These changes are particularly important at $T_{\text{eff}} \lesssim 8\text{kK}$; for models at $T_{\text{eff}} \gtrsim 10\text{kK}$ the differences between the current models, those of Castelli & Kurucz (2004), and the older Kurucz (1993) grids, are small, and result largely from revisions to adopted abundances.

As far as specific intensities are concerned, differences between the newer calculations and older results are illustrated by a comparison between the extensive listings provided by Claret (2000) and the ATLAS9.A10 models pre-

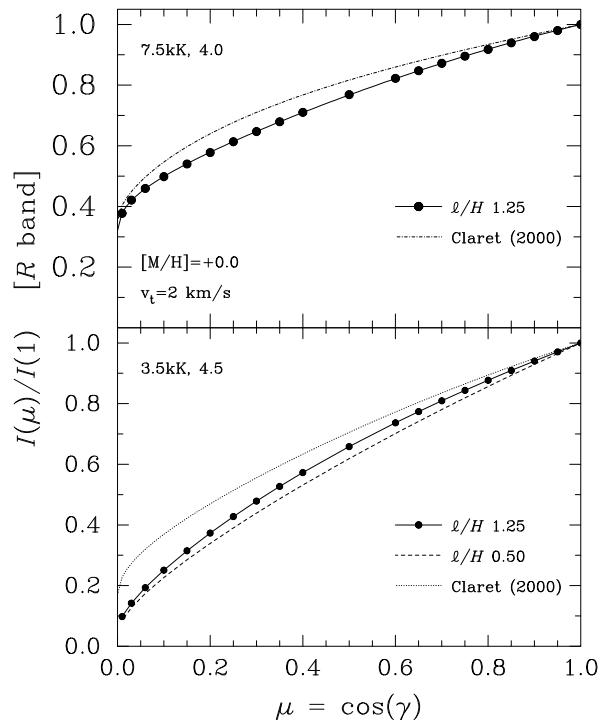


Figure 5. Normalized R -band intensities from the present calculations for two $T_{\text{eff}}/\log g$ values. Filled circles are calculated intensities, and continuous lines the corresponding four-coefficient fits. The Claret (2000) results characterize earlier ATLAS9 models.

sented here (Fig. 4). The changes can be much larger than any that arise through different fitting techniques, provided that the adopted functional form is adequate (Fig. 5).

We might expect further developments in ATLAS models in future, but there is reason to hope that consequences may be modest in scale, at least in the short term; using the latest version of his opacity-sampling ATLAS12 code, Kurucz (personal communication) has kindly computed a solar-abundance model at $T_{\text{eff}} = 7.5\text{kK}$, $\log g = 4.0$, $v_t = 2 \text{ km s}^{-1}$. Differences between old and new ATLAS9 models are relatively large for these parameters, but further changes

in the ATLAS12 products are negligible for the present purposes.

Finally, the limitations of the present work should be recognised. First, although the Kurucz/Castelli ODFs used here represent a significant improvement over older compilations, they are still inevitably incomplete. In particular, there are a number of indications that ATLAS9 models begin to show significant disagreement with observations for effective temperatures $\lesssim 4\text{kK}$ (e.g., Bessell, Castelli & Plez 1998; Bertone et al. 2008), presumably because of the increasing importance of missing molecular opacities. Models at the coolest effective temperatures should be used with caution.

Secondly, the synthetic photometry can be expected to show not only the successes in reproducing observations reported for similar models by Bessell, Castelli & Plez (1998) and Castelli (1999), but also the failures; note that Bessell, Castelli & Plez (1998, cf. their Appendix E.3.1) find that their modelled ($U - B$) colours (i.e., using $U_X - B_X$ passbands) required an ad hoc scaling of $0.96\times$ to bring them into agreement with observations.

Thirdly, it must be owned that the new models presented here fare no better than old ones in matching the handful of apparently reliable empirical determinations of stellar limb darkening (e.g., Heyrovský 2007; Claret 2008, 2009), although such determinations are usually limited to estimates of coefficients for linear or, occasionally, quadratic limb-darkening laws for stars other than the Sun (and such laws are poor representations of model results). Common simplifying model-atmosphere approximations for scattering phase functions will be a factor in this; although such approximations may be appropriate for structure and integrated-flux calculations, they have obvious weaknesses for evaluating intensities (or polarizations). Addressing these issues is a matter for future study.

7 RECOMMENDATIONS

Practically all modern studies in the optical region use photon-counting detectors, and so models appropriate to that context will normally be used. The investigator is still faced with choices in model convection, microturbulence, and abundance (Table 1), and in limb-darkening parameterization (equations 4–8). If, as is frequently the case, there are no results from detailed analyses to suggest otherwise, it's reasonable to adopt the appropriate global abundance system (solar, LMC, or SMC), $v_t = 2 \text{ km s}^{-1}$, $\ell/H = 1.25$. The careful investigator might well conduct sensitivity tests to examine the consequences of other parameters (including varying T_{eff} and $\log g$); in particular, for effective temperatures less than $\sim 8\text{kK}$, it would be prudent to examine the effects of models computed at $\ell/H = 0.50$.

Other than for comparison with empirically-determined limb-darkening laws (normally linear, but increasingly for quadratic coefficients), there is little merit in adopting anything other than a four-coefficient limb-darkening parameterization (equation 8) if seeking an accurate representation of model-atmosphere intensities. The computational cost compared to simpler formulae is trivial in anything other than Monte-Carlo calculations, and even there the overhead should be entirely tolerable.

ACKNOWLEDGMENTS

I gratefully acknowledge the contribution made by R.L. Kurucz in making his codes open source and his datasets freely available, and the work carried out by F. Castelli and her colleagues in porting them to run on GNU-linux systems. I thank Susana Barros, Mike Bessell, Antonio Claret, Steve Fossey, Urtzi Jauregi, Bob Kurucz, Luca Sbordone, Barry Smalley, and the referee for helpful correspondence and comments.

REFERENCES

- Allen, C.W., 1976, *Astrophysical Quantities* (3rd edition), Athlone Press
- Asplund, M., Grevesse, N., Sauval, A.J., 2005, in *Cosmic Abundances as Records of Stellar Evolution and Nucleosynthesis* (ASP Conf. Series 336), 25
- Aufdenberg, J.P., Mérand, A., Coudé du Foresto, V., Absil, O., Di Folco, E., Kervella, P., Ridgway, S.T., Berger, D.H., ten Brummelaar, T.A., McAlister, H.A., Sturmman, J., Sturmman, L., Turner, N.H., 2010., *ApJ*, 645, 664 (erratum 651, 617)
- Aufdenberg, J.P., Ludwig, H.-G., Kervella, P., 2005, *ApJ*, 633, 424
- Aufdenberg, J.P., Ludwig, H.-G., Kervella, P., 2005, *ApJ*, 633, 424
- Barban, C., Goupil, M.J., Van't Veer-Menneret, C., Garrido, R., Kupka, F., Heiter, U., 2003, *A&A*, 405, 1095
- Barry, D.C., 1969, *PASP*, 81, 339
- Bertone, E., Buzzoni, A., Chávez, M., Rodríguez-Merino, L.H., 2008, *A&A*, 485, 823
- Bessell, M.S., 1990, *PASP*, 102, 1181
- Bessell, M.S., 2000, *PASP*, 112, 961
- Bessell, M.S., 2005, *ARA&A*, 43, 293
- Bessell, M.S., Brett, J.M., 1988, *PASP*, 100, 1134
- Bessell, M.J., Castelli, F., Plez, B., 1998, *A&A*, 333, 231 (erratum 337, 321)
- Bohlin, R.C., 2007, in *The Future of Photometric, Spectrophotometric and Polarimetric Standardization* (ASP Conference Series, no. 364) p. 315
- Bonanos, A.Z., 2009, *ApJ*, 691, 407
- Castelli, F., Kurucz, R.L., 2004, in *Modelling of Stellar Atmospheres* (IAU Symp. 203), p. A20 (astro-ph/0405087)
- Castelli, F., Kurucz, R.L., 1994, *A&A*, 281, 817
- Castelli, F., 1999, *A&A*, 346, 564
- Castelli, F., 2005, *MemSAI Sup.*, 8, 34
- Castelli, F., Gratton, R.G., Kurucz, R.L., 1997, *A&A*, 318, 841 (erratum 324, 432)
- Ciardi, D.R., van Belle, G.T., Akeson, R.L., Thompson, R.R., Lada, E.A., Howell, S.B., 2001, *ApJ*, 559, 1147
- Claret, A., 2000, *A&A*, 363, 1081
- Claret, A., 2008, *A&A*, 482, 259
- Claret, A., 2009, *A&A*, 506, 1335
- Cohen, M., Walker, R.G., Barlow, M.J., Deacon, J.R., 1992, *AJ*, 104, 1650
- Crawford, D.L., Barnes, J.V., 1970, *AJ*, 75, 978
- Crawford, D.L., Barnes, J.V., Golson, J.C., 1970, *AJ*, 75, 624
- Díaz-Cordovés, J., Giménez, A., 1992, *A&A*, 259, 227
- Evans, C., Hunter, I., Smartt, S., Lennon, D., de Koter, A., Mokiem, R., Trundle, C., Dufton, P., Ryans, R., Puls, J., Vink, J., Herrero, A., Simón-Daz, S., Langer, N., Brott, I., 2008, *The Messenger*, no. 131, 25

- Fabregat, J., Reig, P., 1996, *PASP*, 108, 90
- Fischer, D.A., Valenti, J. 2005, *ApJ*, 622, 1102
- Garnett, D.R., 1999, in *New Views of the Magellanic Clouds (IAU Symp. 190)*, p. 266
- Glushneva, I.N., Kharitonov, A.V., Kniazeva, L.N., Shenavrin, V.I., 1992, *A&AS*, 92, 1
- Gonzalez, G. 1997, *MNRAS*, 285, 403
- Gray, R.O., 1988, *JRASC*, 82, 336
- Gray, R.O., 1998, *AJ*, 116, 482
- Grevesse, N., Sauval, A.J., 1998, *Space Sci. Rev.*, 85, 161
- Grygar, J., Cooper, M.L., Jurkevuch, I., *BAICz*, 23, 147
- Gulliver, A.F., Adelman, S.J., Cowley, C.R., Fletcher, J.M., *ApJ*, 380, 223
- Hamamatsu Photonics, 1999, Photomultiplier Tube 1P21 data sheet,
http://sales.hamamatsu.com/assets/pdf/parts_R1P21.pdf
- van Hamme, W., 1993, *AJ*, 106, 2096
- Harries, T.J., Hilditch, R.W., Howarth, I.D., 2003, *MNRAS*, 339, 157
- Hayes, D.S., 1985, in *Calibration of Fundamental Stellar Quantities (IAU Symp. 111)*, p. 225
- Hestroffer, D., 1997, *A&A*, 327, 199
- Hewett, P.C., Warren, S.J., Leggett, S.K., Hodgkin, S.T., *MNRAS*, 367, 454
- Heyrovský, D., 2007, *ApJ*, 656, 483
- Hilditch, R.W., Howarth, I.D., Harries, T.J., 2005, *MNRAS*, 357, 304
- Hill, G., Gulliver, A.F., Adelman, S.J., 2010, *ApJ*, 712, 250
- Hill, G.M., Landstreet, J.D., 1993, *A&A*, 276, 142
- Hill, V., Andrievsky, S., Spite, M., 1995, *A&A*, 293, 347
- Hill, V., *A&A*, 324, 435
- Hunter, I., Dufton, P.L., Smartt, S.J., Ryans, R.S.I., Evans, C.J., Lennon, D.J., Trundle, C., Hubeny, I., Lanz, T., 2007, *A&A*, 466, 277
- Jeans J.H., 1917, *MNRAS*, 78, 28
- Johansen, K.T., Gyldenkerne, K., 1970, 1970, *A&AS*, 1, 165
- Johnson, H.L., Iriarte, B., Mitchell, R.I., Wisniewski, W.Z., *Comm. Lunar and Planetary Lab.*, 4, 99
- Klinglesmith, D.A., Sobieski, S., 1970, *AJ*, 75, 175
- Kopal, Z., 1949, *HCO Circ.* 454
- Kurucz, R.L., 1979, *ApJS*, 40, 1
- Kurucz, R.L., 1993, CD-ROM 12, Smithsonian Astrophysical Observatory
- Kurucz, R.L., 1996, in *Model Atmospheres and Spectrum Synthesis (ASP Conf. Series 108)*, 2
- Kurucz, R.L., 2005, *MemSAI Sup.*, 8, 76
- Luck, R.E, Moffett, T.J., Barnes, T.G., III; Gieren, W.P., *AJ*, 115, 605
- Manduca, A., Bell, R.A., Gustafsson, B., 1977, *A&A*, 61, 809
- Mégessier, C., 1995, *A&A*, 296, 771
- Milne E.A., *MNRAS* 81, 361
- Mokiem, M.R., de Koter, A., Evans, C.J., Puls, J., Smartt, S.J., Crowther, P.A., Herrero, A., Langer, N., Lennon, D.J., Najarro, F., Villamariz, M.R., Vink, J.S., 2007, *A&A*, 465, 1003
- North, P.L., Gauderon, R., Barblan, F., Royer, F., 2010, *A&A*, 520, 74
- Perry, C.L., 1969, *AJ*, 74, 139
- Praezisions Glas & Optik GmbH data sheet,
http://www.pgo-online.com/intl/katalog/curvesBK7_kurve.html
- Qiu, H.M., Zhao, G., Chen, Y.Q., Li, Z.W., 2001, *ApJ*, 548, 953
- Russell, H.N., 1912, *ApJ*, 35, 315
- Russell, H.N., Shapley, H., 1912, *ApJ*, 36, 239
- Russell, S.C., Dopita, M.A., 1992, *ApJ*, 384, 508
- Sbordone, L., Bonifacio, P., Castelli, F., 2007, in *Convection in Astrophysics (IAU Symp. 239)*, p. 71
- Schwarzschild K., 1906, *Nachrichten von der Gesellschaft der Wissenschaften zu Göttingen, Mathematisch-Physikalische Klasse*, p. 43
- Smalley, B., 2005, *MemSAI Sup.*, 8, 155
- Southworth, J., 2008, *MNRAS*, 386, 1644
- Sousa, S.G., Santos, N.C., Mayor, M., Udry, S., Casagrande, L., Israelian, G., Pepe, F., Queloz, D., Monteiro, M.J.P.F.G., 2008, *A&A*, 487, 373
- Stubbs, C.W., High, F.W., George, M.R., DeRose, K.L., Blondin, S., Tonry, J.L., Chambers, K.C., Granett, B.R., Burke, D.L., Smith, R.C., 2007, *PASP*, 119, 1163
- Taylor, B.J., *ApJS*, 54, 259
- Trundle, C., Dufton, P.L., Hunter, I., Evans, C.J., Lennon, D.J., Smartt, S.J., Ryans, R.S.I., 2007, *A&A*, 471, 625
- van 't Veer, F., 1960, *Recherches Astronomiques de l'Observatoire d'Utrecht*, 14, no. 3
- van Noord, M., Lanz, T., Lamers, H.J.G.L.M., Kurucz, R.L., Ferlet, R., Hebrard, G., Vidal-Madjar, A., 1998, *A&A*, 334, 633
- Venn, K.A., 1999, *ApJ*, 518, 405
- Wade, R.A., Rucinski, S.M., 1985, *A&AS*, 60, 471
- Wilson, R., 1990, *ApJ*, 356, 613
- Witt, H.J., *ApJ*, 449, 42

Table A1. Adopted LMC and SMC abundances, by number, on a scale where the hydrogen abundance is 12.0 dex.

Element	LMC	SMC	Element	LMC	SMC	Element	LMC	SMC	Element	LMC	SMC				
2	He	10.88	10.85	24	Cr	5.43	5.06	46	Pd	1.39	1.09	68	Er	0.63	0.33
3	Li	0.75	0.45	25	Mn	5.06	4.88	47	Ag	0.64	0.34	69	Tm	-0.30	-0.60
4	Be	1.08	0.78	26	Fe	7.23	6.93	48	Cd	1.47	1.17	70	Yb	0.78	0.48
5	B	2.40	2.10	27	Co	4.62	4.32	49	In	1.30	1.00	71	Lu	-0.24	-0.54
6	C	7.73	7.37	28	Ni	6.02	5.82	50	Sn	1.70	1.40	72	Hf	0.58	0.28
7	N	6.90	6.50	29	Cu	3.91	3.63	51	Sb	0.70	0.40	73	Ta	-0.47	-0.77
8	O	8.35	7.98	30	Zn	4.20	4.00	52	Te	1.89	1.59	74	W	0.81	0.51
9	F	4.26	3.96	31	Ga	2.58	2.28	53	I	1.21	0.91	75	Re	-0.07	-0.37
10	Ne	7.60	7.20	32	Ge	3.28	2.98	54	Xe	1.97	1.67	76	Os	1.15	0.85
11	Na	6.97	5.78	33	As	1.99	1.69	55	Cs	0.77	0.47	77	Ir	1.08	0.78
12	Mg	7.06	6.72	34	Se	3.03	2.73	56	Ba	1.94	1.23	78	Pt	1.34	1.04
13	Al	6.07	6.27	35	Br	2.26	1.96	57	La	1.06	0.84	79	Au	0.71	0.41
14	Si	7.19	6.79	36	Kr	2.98	2.68	58	Ce	1.45	1.26	80	Hg	0.83	0.53
15	P	5.06	4.76	37	Rb	2.30	2.00	59	Pr	0.41	0.11	81	Tl	0.60	0.30
16	S	6.70	6.30	38	Sr	2.46	1.32	60	Nd	1.66	1.47	82	Pb	1.70	1.40
17	Cl	5.01	4.95	39	Y	1.88	1.60					83	Bi	0.35	0.05
18	Ar	6.20	5.90	40	Zr	2.20	1.93	62	Sm	0.98	1.13				
19	K	4.78	4.48	41	Nb	1.12	0.82	63	Eu	0.22	0.25	90	Th	-0.24	-0.54
20	Ca	5.83	5.63	42	Mo	1.62	1.32	64	Gd	0.82	0.52				
21	Sc	2.62	2.31					65	Tb	-0.02	-0.32	92	U	-0.82	-1.12
22	Ti	4.63	4.31	44	Ru	1.54	1.24	66	Dy	0.84	0.54				
23	V	4.10	3.56	45	Rh	0.82	0.52	67	Ho	0.21	-0.09				

APPENDIX A: ADOPTED MAGELLANIC-CLOUD ABUNDANCES

Baseline solar abundances were taken from Asplund, Grevesse & Sauval (2005). Cloud abundances were adopted, in order of preference, from: FLAMES results (Hunter et al. 2007, Trundle et al. 2007, as summarized by Evans et al. 2008); Garnett (1999); and Russell & Dopita (1992, applying their differential values to Asplund solar abundances). In each case, samples of early-type stars or H II regions were analysed, so the abundances are representative of Population I. For elements not studied in these sources, solar abundances were used, adjusted by the median metal offsets from Russell & Dopita (1992): -0.3 (LMC) and -0.6 dex (SMC). These global adjustments are in adequate agreement with more-recent discussions (e.g., Hill, Andrievsky & Spite 1995; Hill 1997; Luck et al. 1998; Venn 1999; Mokiem et al. 2007).

APPENDIX B: ON-LINE MATERIAL

New opacity-distribution functions using the Asplund, Grevesse & Sauval (2005) solar abundances are provided on-line, at metallicities $[M/H] = -0.5, +0.0, +0.2, +0.3, +0.4, +0.5$, together with the LMC and SMC ODFs. In each case, ODFs are given sampled at the standard ‘big’ and ‘little’ wavelength sampling intervals required for use with ATLAS9, and for microturbulent velocities of 0, 1, 2, 4, and 8 km s⁻¹, together with the corresponding Rosseland-opacity files. These are binary files in the format required by ATLAS9.

Limb-darkening and flux data products are organized into directories corresponding to the grids listed in Table 1 (for both new models, and those of Castelli & Kurucz 2004). Within a given directory, there are three plain-text files for each model, with names of the form `t05000g40.<ext>` where the base identifies T_{eff} and $\log g$, and the extension identifies the file content.

Files with `.flx` extensions contain listings of physical fluxes at 1221 wavelengths, from 90Å to 160μm (with 20-Å sampling through the optical). Fluxes are tabulated in erg cm⁻² s⁻¹ Å⁻¹ as a function of wavelength (in Å).

Limb-darkening coefficients are provided in files with extensions `.ucP` (for photon-counting detectors; Section 4.1) and `.ucE` (for energy-integrating detectors). The `.ucE` files list broad-band limb-darkening coefficients for Strömgren and Johnson systems (including U_X and B_X passbands for computing synthetic $(U - B)$ colours), while the `.ucP` files give broad-band limb-darkening coefficients for all 30 passbands listed in Section 4.1, plus [energy-integrated] bolometric coefficients. The data given for each passband may be illustrated by V -band results for a Vega model ($T_{\text{eff}} = 9.55\text{kK}$, $\log g = 3.95$, $[M/H] = -0.5$, $v_t = 2 \text{ km s}^{-1}$, $\ell/H = 1.25$):

Bessell-V	5467.7	5.61840E+07	2.08372E+07	-0.207		
4-coeff	+4.73679E-01	+5.53030E-01	-5.01375E-01	+1.56613E-01	+2.75266E-04	-7.09332E-04
quadratic	+2.25617E-01	+3.71954E-01			+1.56919E-02	-4.19850E-02
quad - FC	+2.74255E-01	+3.01889E-01			+1.82965E-02	-6.25047E-02
square root	+2.25306E-02	+6.82355E-01			+2.77154E-03	+6.52661E-03
logarithmic	+6.36370E-01	+3.25055E-01			+5.45636E-03	-1.48612E-02
linear - 2	+1.04831E+00	+5.92481E-01			+3.77170E-02	-9.16531E-02
linear - 1	+5.25808E-01				+4.55362E-02	-1.09348E-01
linear - FC	+4.25199E-01				+7.68496E-02	-2.08951E-01

Here the first line lists

- (i) the passband,
- (ii) effective wavelength (in Å),
- (iii) the broad-band physical flux $f(\lambda)$ (in erg cm⁻² s⁻¹ Å⁻¹),
- (iv) the broad-band surface-normal intensity $I_\lambda(1)$ (in erg cm⁻² s⁻¹ Å⁻¹ sr⁻¹), and
- (v) the bolometric correction (for Johnson passbands only).

Subsequent lines list coefficients for the limb-darkening laws summarized in Section 4.2; the final two numbers in each row are the r.m.s. and maximum differences between input and modelled values of $I(\mu)/I(1)$.

The ‘linear - FC’ and ‘quad - FC’ results use flux conservation in place of least squares, with the fitted value $\hat{I}(1)$ anchored to the model $I(1)$ in the first case, and additionally $\hat{I}(0.1)$ to $I(0.1)$ in the second (cf. Wade & Rucinski 1985). The ‘linear - 1’ listing is for the standard (single-parameter) least-squares fit to eqtn. (4), while the coefficients in the ‘linear - 2’ listing are for a model with $\hat{I}(1)$ free, i.e.,

$$I(\mu)/I(1) = a - b(1 - \mu).$$

This paper has been typeset from a $\text{T}_\text{E}\text{X}/\text{L}^\text{A}\text{T}_\text{E}\text{X}$ file prepared by the author.